



ELSEVIER

Available online at [www.sciencedirect.com](http://www.sciencedirect.com)

SCIENCE @ DIRECT®

Earth and Planetary Science Letters 213 (2003) 337–345

EPSL

[www.elsevier.com/locate/epsl](http://www.elsevier.com/locate/epsl)

# Some additional parameters to estimate domain state from isothermal magnetization measurements

Karl Fabian\*

*Universität Bremen, FB Geowissenschaften, Postfach 330440, 28334 Bremen, Germany*

Received 6 January 2003; received in revised form 26 May 2003; accepted 3 June 2003

## Abstract

Domain state and mixing analysis based on isothermal magnetization measurements is often restricted to the use of the Day plot. In order to make more information from simple rock magnetic measurements accessible for the quantitative analysis of domain state, four additional parameters are proposed. Two of them, a hysteresis shape parameter and a coercivity ratio, can be directly calculated from standard measurements of the hysteresis loop and backfield curve. The other two, a transient energy dissipation ratio and the viscosity of isothermal remanent magnetization, require additional measurements, which, however, do not increase measurement time noticeably. The theoretical background of the above parameters is discussed. Their ability to discern domain state is shown for a small set of synthetic magnetite and titanomagnetite samples and in a case study of a transect from the rim to the center of a dredged mid-ocean ridge basalt.

© 2003 Elsevier B.V. All rights reserved.

*Keywords:* rock magnetism; hysteresis

## 1. Introduction

In rock and environmental magnetism isothermal magnetization measurements provide the most simple and fundamental quantities to estimate domain state of the remanence carriers. The notion of isothermal magnetization measurement subsumes a number of very different measurement procedures. All types of hysteresis measurements, including initial curve and minor loops as well as remanence measurements and even time

dependent measurements belong to this group. Isothermal measurements are especially convenient, because they can be performed fast and easily even on large sample sets. In the following the terminology and notation of [1] are used. The standard procedure to estimate domain state in rock magnetism is the Day plot [2]. It is based on the measurement of two isothermal magnetization curves. The hysteresis loop consisting of an upper branch  $M^+(B)$  and a lower branch  $M^-(B)$  as well as the backfield curve  $M_{bf}(B)$ . From this large set of measurements, only four parameters are extracted: The saturation magnetization  $M_s$  is usually approximated by interpreting the high field slope of  $M^+(B)$  as representing the paramagnetic susceptibility, which then is subtracted from

\* Tel.: +49-421-218-3938; Fax: +49-421-218-7008.

E-mail address: [karl.fabian@uni-bremen.de](mailto:karl.fabian@uni-bremen.de) (K. Fabian).

both hysteresis branches to obtain the ferro- or ferrimagnetic loop. By definition,  $M_s$  is the high field asymptotic value of the latter. A more refined technique to extrapolate for  $M_s$  using an approach to saturation law has been proposed in [3]. The second value is the saturation remanence  $M_{rs}$  defined as  $M^+(0)$ . The ratio  $M_{rs}/M_s$  is high, if the sample is not able to demagnetize itself by the action of its self-induced magnetostatic – or self-demagnetizing – field. High  $M_{rs}/M_s$  is therefore indicative of single-domain (SD) or pseudo-single-domain (PSD) particles as remanence carriers. On the other hand, low  $M_{rs}/M_s$  indicates effective self-demagnetization. This occurs either by formation of magnetic domains for large multi-domain (MD) remanence carriers or by thermally activated magnetization reversal if superparamagnetic (SP) particles are abundant. Further, the coercive force  $B_c$ , defined by  $M^-(B_c)=0$ , and the coercivity of remanence  $B_{cr}$ , defined by  $M_{bf}(B_{cr})=0$ , are obtained from the measured magnetization curves. The ratio  $B_{cr}/B_c$  again is indicative of domain state. The theoretical value for an isotropic ensemble of uniaxial non-interacting SD particles is 1.09 [4], for large MD magnetite,  $B_{cr}/B_c \geq 5$ .

Often, rock and environmental studies confine the quantitative domain state interpretation of their isothermal measurement curves to the Day plot, which incorporates only the above ratios  $M_{rs}/M_s$ ,  $B_{cr}/B_c$ . Although indeed a lot of information about domain state and mixing can be directly or indirectly inferred from the Day plot [5,6], there still is much additional information left in the original data set  $M^\pm(B)$ ,  $M_{bf}(B)$ , which can help to resolve the often remaining ambiguities in practical applications. There exist quite a number of interesting and valuable approaches to use this remaining information. Mathematical analysis of hysteresis loops allows to infer Fourier expansions [7] or coercivity spectra [3] which contain the complete information about the loops. Additional measurement of a dense set of first order reversal curves yields a two-dimensional picture of a special switching field distribution of the sample [8,9]. There exists extensive literature about hysteresis modelling in the material sciences, but their aim is to understand and model

the hysteresis properties of well-defined homogeneous materials. In applied rock magnetism, isothermal magnetization measurements are used as diagnostic tools to interpret the properties of complex mineral and grain-size mixtures. This requires to represent the additional information by robust quantitative parameters which have a clear physical meaning independent of very special assumptions about mineralogy and grain size. In this respect, the suitability of some additional hysteresis parameters, partly suggested in [10], has already been tested in [11].

Here, another four quantitative parameters are presented. They also are partly based on previous studies [1,12]. Two of them – the shape parameter  $\sigma_{\text{hys}}$  and the coercivity ratio  $B_{rh}/B_{cr}$  – allow to extract additional information from the standard isothermal data sets of  $M^\pm(B)$ ,  $M_{bf}(B)$ . Their information content is not directly related to  $M_{rs}/M_s$  and  $B_{cr}/B_c$ , although  $B_{rh}/B_{cr}$  is also indicative of domain state. Moreover, two simple extensions of the classical isothermal measurement scheme are proposed, which allow for even more detailed domain state investigation, without noticeably increasing experimental effort or measurement duration. They involve the measurement of an additional hysteresis branch  $M_{si}(B)$  and the inclusion of an estimate of viscosity of isothermal remanent magnetization (VIRM).

## 2. Transient energy dissipation (TED)

From a physical point of view, the most easily accessible parameter proposed here is TED.

The essential physical difference between SD and MD particles is that the self-induced magnetostatic field in MD particles is sufficient to partially demagnetize the particle by *irreversible* processes such as domain wall nucleation or domain wall pinning by inclusions or defects. Note that *reversible* demagnetization due to spin rotation or thermally activated switching – as in SP particles – occurs also in SD ensembles and is responsible for ambiguity in  $M_{rs}/M_s$ .

The slightly extended hysteresis measurement scheme proposed in [1] and shown in Fig. 1 allows to determine exactly the energy which is dissi-

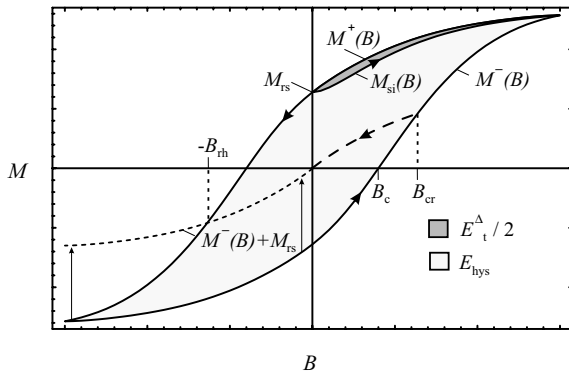


Fig. 1. Extended hysteresis measurement including determination of the  $M_{si}$  curve. The dark shaded area corresponds to half of  $E_t^\Delta$ . The other half is contained in the symmetric curve at negative fields. The total area between the lower hysteresis branch  $M^-(B)$  and the upper branch  $M^+(B)$  is denoted by  $E_{hys}$ . Also indicated are the definitions of  $M_{rs}$ ,  $B_c$ ,  $B_{cr}$  and  $B_{rh}$ .

pated by the above *irreversible* self-demagnetization processes. The measurement is performed in the following way:

1. Apply  $B = B_{max}$  and then set  $B = 0$  to prepare the sample in the state of saturation remanence  $M_{rs}$ . In order to avoid overshooting to negative fields in our alternating gradient field magnetometer it turned out to be useful to reset the field to zero in two or three steps (10, 1 and 0 mT).
2. Measure initial curve plus hysteresis loop starting from this state. The thus obtained 'initial curve' is the *saturation initial curve*  $M_{si}(B)$  [1].

The energy:

$$E_t^\Delta = 2 \int_0^{B_{max}} (M^+(B) - M_{si}(B)) dB \quad (1)$$

is dissipated solely by transient irreversible processes initiated by the action of the self-demagnetizing field of the sample. In a sufficiently high maximal field  $B_{max}$  all magnetic spins are nearly aligned with the field. Only reversible rotations or para-processes occur at high fields. Reducing the field to  $B = 0$  along the magnetization curve  $M^+(B)$  results in domain nucleation and wall movement if the self-demagnetizing field is strong enough in comparison to magnetocrystalline ani-

sotropy, exchange energy and magnetostriction. Increasing the field back to  $B_{max}$  along the magnetization curve  $M_{si}(B)$  reverses the above processes. Yet, in PSD and MD remanence carriers wall pinning and nucleation failure lead to a gap between  $M^+(B)$  and  $M_{si}(B)$ . The area  $E_t^\Delta$  of this gap is equivalent to half the TED initiated solely by the action of the self-demagnetizing field. The factor 2 in Eq. 1 takes into account the symmetric processes for negative field values.

The ratio between  $E_t^\Delta$  and the total hysteresis area:

$$E_{hys} = \int_{-B_{max}}^{B_{max}} (M^+(B) - M^-(B)) dB \quad (2)$$

determines which fraction of the total energy dissipation is related to TED. In ideal non-interacting SP–SD mixtures  $E_t^\Delta = 0$  since in both constituents no irreversible processes are induced by the self-demagnetizing field. As long as  $E_{hys} \neq 0$ , also the ratio  $E_t^\Delta/E_{hys}$  is zero for these mixtures. Due to magnetostatic interaction  $E_t^\Delta/E_{hys}$  in real SP–SD ensembles deviates from zero. However, samples with  $E_t^\Delta/E_{hys} < 5\%$  can safely be interpreted as interacting SP–SD mixtures. In MD samples  $E_t^\Delta/E_{hys}$  can rise above 50% as shown in Fig. 2.

The most important property of  $E_t^\Delta/E_{hys}$  is that it varies continuously with grain size over the whole SD–MD spectrum. Most notably, it is not influenced by SP grain-size fractions, since no irreversible processes occur in SP particles. In this respect, the TED ratio  $E_t^\Delta/E_{hys}$  is less ambiguous than  $M_{rs}/M_s$ , which cannot discriminate between reversible and irreversible self-demagnetization. Therefore,  $M_{rs}/M_s$  decreases with increasing grain size, but also with increasing SP content. Of course, as with  $M_{rs}/M_s$ , it is neither possible to discriminate mixtures of SD and MD particles from PSD particles by  $E_t^\Delta/E_{hys}$ , nor is it possible to distinguish chemical alteration and changes of internal stress from grain-size variation. Yet, it is a most reasonable parameter for average 'magnetic grain size'.

### 3. A coercivity ratio related to TED

It is possible to derive coercivity related ratios

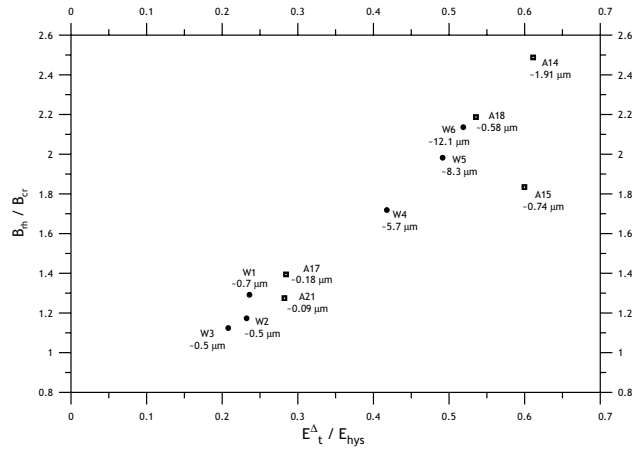


Fig. 2. The ratio  $B_{rh}/B_{cr}$  in dependence on TED  $E_t^\Delta/E_{hys}$  for synthetic magnetite and titanomagnetite samples. The magnetite samples W1–W6 are produced by Wright Industries and described in [13]. The titanomagnetite samples A14, A15, A17, A18 and A21 are described in [14]. The linear relationship between the two ratios shows that  $B_{rh}/B_{cr}$  is well suited as a domain state indicator.

which also reflect TED [1]. Especially the ratio  $B_{rh}/B_{cr}$  is useful in this respect since it can be determined from standard magnetization measurements  $M^\pm(B)$ ,  $M_{bf}(B)$ . By definition [10,3],  $B_{rh}$  is the median destructive field of the vertical hysteresis difference:

$$M_{rh}(B) = \frac{M^+(B) - M^-(B)}{2} \quad (3)$$

In [11] it has been denoted by  $MDF_{hys}$ . Graphically,  $B_{rh}$  is the positive field value where the difference between upper and lower hysteresis branches has decreased from  $2M_{rs}$  at  $B=0$  to  $M_{rs}$  or where the upper hysteresis branch intersects with the lower branch after shifting the latter upward by  $M_{rs}$ . It has been shown in [1] that for samples with stable positive Preisach function  $B_{rh}/B_{cr} \geq 1$ , and that an approximative calculation yields:

$$B_{rh}/B_{cr} \approx 1 + \frac{M^+(B_{rh}) - M_{si}(B_{rh})}{M_{rs}} \quad (4)$$

This estimate relates  $B_{rh}/B_{cr}$  to the gap between  $M^+(B)$  and  $M_{si}(B)$  and consequently to the ratio  $E_t^\Delta/E_{hys}$ . Thus, high  $B_{rh}/B_{cr}$  ratios indicate prevalence of transient irreversible processes and therefore large particles. On the other hand, in natural ensembles containing SP particles  $B_{rh}/B_{cr}$  ratios below 1 are observed as will be seen in Section

6. This indicates that mixtures containing both SP and SD particles are not well described by a stable positive Preisach function. A possible explanation is predominant negative interaction effects between stable SD and SP particles. Yet, the above behavior of  $B_{rh}/B_{cr}$  is extremely useful for domain state analysis, since it clearly separates SP, SD and MD domain states by a single easily determined parameter. The linear relationship between  $B_{rh}/B_{cr}$  and  $E_t^\Delta/E_{hys}$  in Fig. 2 provides evidence that  $B_{rh}/B_{cr}$  indeed is indicative of domain state. Yet, it must be emphasized that  $E_t^\Delta/E_{hys}$  has a direct physical meaning which shows that it is linked to domain state, whereas  $B_{rh}/B_{cr}$  is an inferred quantity, the physical interpretation of which is not equally clear.  $B_{rh}/B_{cr}$  can serve as a substitute for  $E_t^\Delta/E_{hys}$  for the extended interpretation of already existing hysteresis loops. However, it is recommended to rely on  $E_t^\Delta/E_{hys}$  when the necessary measurement of  $M_{si}(B)$  is possible.

#### 4. Quantifying hysteresis shape

Shape anomalies of hysteresis loops are frequently interpreted as being indicative of SP particles [15] or more generally for mixtures of fractions with highly contrasting coercivities [16,17]. There are few attempts to quantitatively use hys-

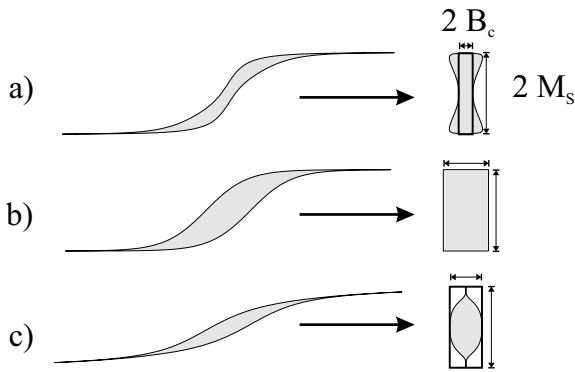


Fig. 3. A simple way to quantify the shape of a hysteresis loop is to compare the area  $E_{\text{hys}}$  with an ideal rectangular area. A hypothetical ideal loop ( $B$ ) consists of two congruent branches which cross the  $B$  axis at  $-B_c$  and  $+B_c$ , respectively. The horizontal distance between the branches at each magnetization is  $2B_c$ , thus the total area is  $2B_c \times 2M_s$ . In case of a ‘wasp-waisted’ loop (a), the area  $E_{\text{hys}}$  is larger than  $4M_s B_c$ , whereas for ‘potbellied’ loops (c)  $E_{\text{hys}} < 4M_s B_c$ . The areas on the right show symmetric plots of the horizontal width  $B(M)$  obtained by subtracting the hysteresis branches horizontally.

teresis shape information. The  $ww$  factor of [18,19] allows to assess the constriction of the hysteresis loop, but cannot discriminate among non-constricted (‘potbellied’) loops, which all have  $ww = 1$ . Consequently, only very inhomogeneous mixtures with large content of both constituents are detectable and  $ww$  varies extremely non-linearly with mixing ratio. Here the following more linearly behaving and more sensitive shape parameter  $\sigma_{\text{hys}}$  is advertised. It is defined by:

$$\sigma_{\text{hys}} = \log\left(\frac{E_{\text{hys}}}{4M_s B_c}\right) \quad (5)$$

where  $\log$  represents the natural logarithm. The shape parameter  $\sigma_{\text{hys}}$  compares the actual area  $E_{\text{hys}}$  of the hysteresis loop with the rectangular area with height  $2M_s$  and width  $2B_c$ . The latter area corresponds to an ‘ideal’ hysteresis loop having two congruent branches, one passing through zero at  $-B_c$ , the other at  $+B_c$ . As shown in Fig. 3, for wasp-waisted loops  $E_{\text{hys}} > 4M_s B_c$  and accordingly  $\sigma_{\text{hys}} > 0$ , whereas for potbellied loops  $E_{\text{hys}} < 4M_s B_c$  and  $\sigma_{\text{hys}} < 0$ . The logarithmic definition of  $\sigma_{\text{hys}}$  is intended to obtain a relatively linear measure of shape variation from ‘potbel-

lied’ to ‘wasp-waisted’ loops. Since calculation of  $\sigma_{\text{hys}}$  requires only the standard hysteresis loop  $M^\pm(B)$ , it can be easily included in rock and environmental magnetic studies.

In Fig. 4 measurements of  $\sigma_{\text{hys}}$  for a small selection of sized magnetite and titanomagnetite samples are shown. They indicate that  $\sigma_{\text{hys}}$  is relatively independent of grain size within the SD–MD region. This is important because variations in  $\sigma_{\text{hys}}$  are indicative of either admixture of SP particles or for the presence of an independent mineral fraction.

### 5. VIRM

VIRM is measured by monitoring the decay of an IRM acquired in some high field  $B_{\text{max}}$  [20,12]. The temporal evolution of the magnetization is in good approximation given by:

$$M(t) = M_0 - S \log(t/t_0) \quad (6)$$

Measurement of  $M(t)$  over some reasonable time interval allows to determine the normalized value  $S/M_0$  which is indicative of the presence of magnetizations with relaxation times near  $t_0$ . This is related to the frequency dependence of susceptibility in the vicinity of the frequency  $1/t_0$ . High  $S/M_0$  is indicative of grain sizes close to the transition from SP to stable SD grains. Usually a 100 s

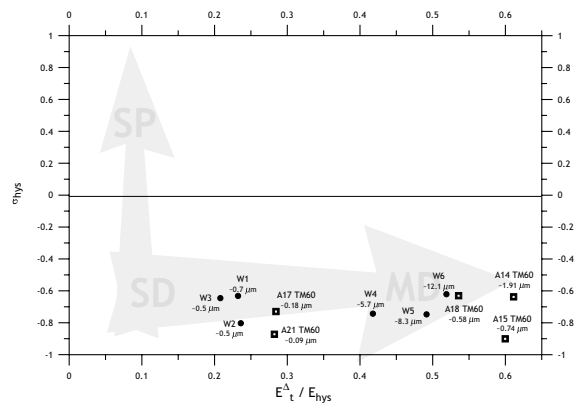


Fig. 4. Measurement results for a suite of synthetic (titanomagnetite) samples. Independent of grain size and composition, all synthetic samples show  $\sigma_{\text{hys}}$  values in the range from  $-0.9$  to  $-0.5$ .  $E_t^\lambda/E_{\text{hys}}$  varies continuously with grain size, but apparently is increased by magnetostatic interaction.

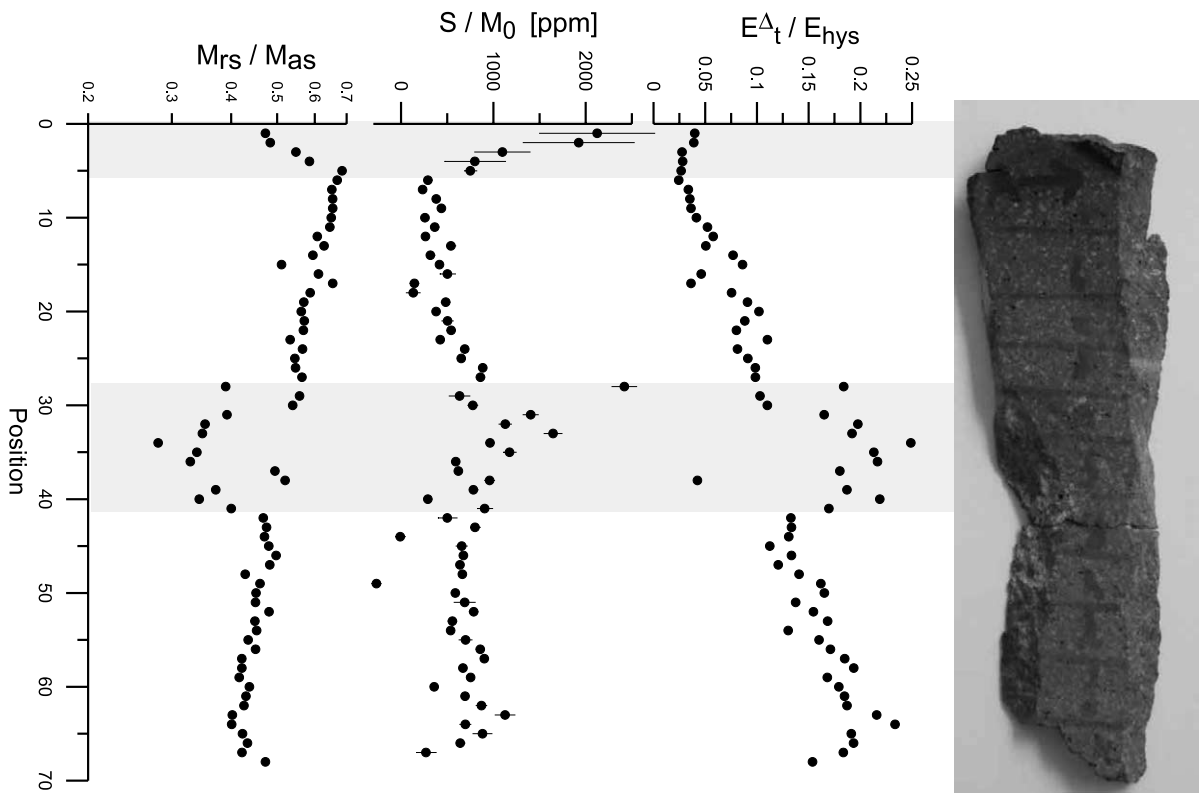


Fig. 5. Cross-section of hysteresis parameters along a zero age MOR basalt T787-R1 (sample provided by D. Kent). Sample position varies only approximately linearly with distance from the chilled margin. The total length of the MORB specimen is 12 cm. As shown by Gee and Kent [19], the grain size increases steadily from SP–SD mixtures at the chilled margin to PSD–MD particles.  $M_{as}$  denotes the ‘apparent’ saturation magnetization as obtained by subtracting the average slope of the hysteresis loop above 70% of the maximum field (here 1 T).

VIRM measurement can be easily included into a hysteresis measurement scheme. Experimental experience, however, shows that VIRM measurements, e.g. using the ‘magnetization versus time’ option of the MicroMag (Princeton Measurement Inc.), often result in very noisy data, since the signal is very small and any vibrations due to air movement or other external influences induce spurious oscillations in the magnetization curve. Such oscillations must be discarded and often only the first few measurement points can be used to estimate  $S/M_0$  and large error margins have to be taken into account. Still it is recommended to add this simple measurement to the standard laboratory routine, because noisy data are better than no data and increased viscosity is a valuable indication for the presence of SP

particles. Of course, the best solution is to set up more reliable special equipment for this measurement as suggested in [12].

## 6. A case study of a transect along a mid-ocean ridge basalt (MORB)

As convincingly demonstrated in [19], there is a systematic variation in domain state from SP over SD to PSD/MD along a 12 cm transect from the chilled outer margin of a MORB to its center. Here a densely sampled zero age MORB (sample T787-R1 provided by D. Kent) is used as a case study in order to test this conclusion on the basis of the parameters proposed above. Already the data in Fig. 5 show that the SD–MD trend is



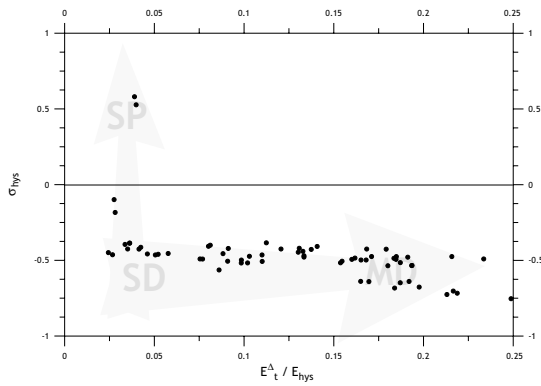


Fig. 6. Plot of  $\sigma_{\text{hys}}$  versus  $E_t^A/E_{\text{hys}}$  for the hysteresis data of the MORB sample T787-R1.

unambiguously represented by  $E_t^A/E_{\text{hys}}$ . Note that this parameter is not influenced by SP fractions. Grain-size variation within the SP–SD transition region is resolved by  $S/M_0$ . The anomalous region between position 28 and 41 is due to an increase of effective grain size, not due to SP admixture. Otherwise  $E_t^A/E_{\text{hys}}$  would not be influenced.

In Fig. 6 shape parameter  $\sigma_{\text{hys}}$  is plotted versus  $E_t^A/E_{\text{hys}}$ , which yields an extremely clear picture of the grain-size variation. Over the whole SD–PSD range,  $\sigma_{\text{hys}}$  varies only slightly around  $-0.5$ , whereas SP-influenced samples have  $\sigma_{\text{hys}}$  values above  $-0.2$ . The lowest  $\sigma_{\text{hys}}$  values occur in the anomalous region of positions 28 through 41. This again discards the possibility of SP admixture which should have increased  $\sigma_{\text{hys}}$ . The decreased values of about  $-0.7$  are closer to the values from the synthetic titanomagnetites of Fig. 4 and therefore rather indicate stress release in the anomalous region. Alternatively,  $\sigma_{\text{hys}}$  may reflect a variation of the oxidation state within the anomalous region and across the transect.

When only data from the standard isothermal measurement  $M^\pm(B)$ ,  $M_{\text{bf}}(B)$  are used, it is still possible to plot  $\sigma_{\text{hys}}$  versus  $B_{\text{rh}}/B_{\text{cr}}$  as in Fig. 7. Here the SP–SD variation is especially clearly resolved, since not only  $\sigma_{\text{hys}}$  increases, but also  $B_{\text{rh}}/B_{\text{cr}}$  adopts values  $< 1$  within this region. Although the SD–PSD transition appears to be less clearly resolved, the variation of  $B_{\text{rh}}/B_{\text{cr}}$  closely mirrors the variation of  $E_t^A/E_{\text{hys}}$  as is shown in the inset of Fig. 7.

According to its physical meaning, the plot of

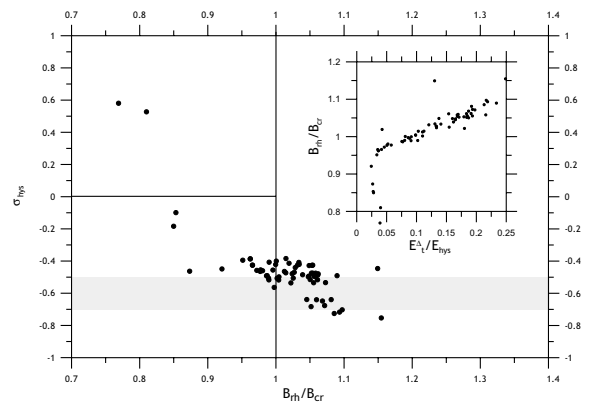


Fig. 7. Plot of the shape parameter  $\sigma_{\text{hys}}$  versus  $B_{\text{rh}}/B_{\text{cr}}$  for the hysteresis data of the MORB sample T787-R1. The inset shows that  $B_{\text{rh}}/B_{\text{cr}}$  varies monotonously with  $E_t^A/E_{\text{hys}}$  in the SD–MD transition region.

viscous IRM versus  $E_t^A/E_{\text{hys}}$  in Fig. 8 traces the presence of low energy barriers in dependence on the presence of transient irreversible processes. In the SD region, viscous processes due to low energy barriers are the hallmark of an SP fraction. Interestingly, there also is a slight but significant increase of  $S/M_0$  with grain size. This indicates that viscous processes in MD grains cannot be completely discarded. This result agrees with the finding of [21] for sized magnetite, but differs from the conclusion of [12]. Comparison with Fig. 5 shows that especially samples from the anomalous region of positions 28–41 have high viscosity values comparable to those in the SP–SD transition region. On its own, viscous IRM as

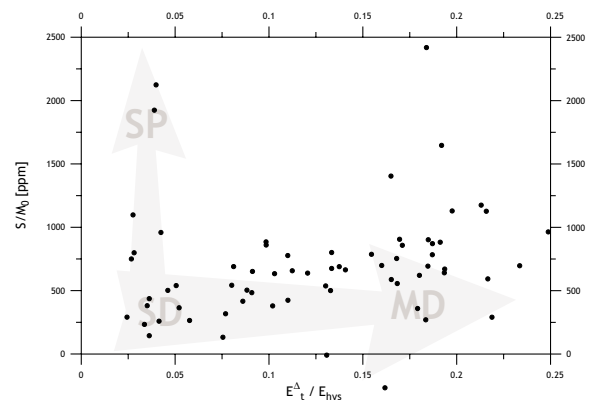


Fig. 8. Viscous IRM versus  $E_t^A/E_{\text{hys}}$  for MORB sample T787-R1.

an SP indicator therefore appears to be more ambiguous than  $\sigma_{\text{hys}}$  or  $B_{\text{rh}}/B_{\text{cr}}$ . In case of complex mineral and grain-size mixtures, a combination of these parameters is the best choice to distinguish an increase of  $\sigma_{\text{hys}}$  due to mineral mixture from an increase effected by an SP fraction.

## 7. Conclusions

A number of additional quantitative parameters from isothermal measurements can help to resolve ambiguities of the Day plot without noticeably increasing measurement effort.

(1) TED is the most direct physical parameter to estimate domain state within the SD–PSD–MD region because it directly measures the irreversible processes due to structural variations during domain formation. It is fast and is easily determined by including an additional branch in the standard hysteresis measurement.

(2) In order to estimate domain state without additional hysteresis data, the coercivity ratio  $B_{\text{rh}}/B_{\text{cr}}$  can be used. It is related to TED, although its physical interpretation is not equally direct.

(3) Hysteresis shape can be quantified by a simple parameter which continuously traces variation from potbellied to wasp-waisted shape of the hysteresis loop. It turns out to be largely independent of grain size within the SD–PSD–MD region and thus serves as an indicator of SP fractions or mineral mixtures.

(4) VIRM also can be included in standard isothermal measurements. The related viscosity parameter is a simple means to detect SP particles in SP–SD mixtures.

## Acknowledgements

The synthetic samples used in this study have kindly been made available by D. Krása and A. Zitzelsberger. I wish to thank D. Kent for providing the MORB sample, L. Tauxe for useful discussions and D. Krüger for help with the measurements. Reviews of D. Dunlop, E. Petrovsky and S. Banerjee and comments of V. Courtillot considerably improved the manuscript. [VC]

## References

- [1] K. Fabian, T. vonDobeneck, Isothermal magnetization of samples with stable Preisach function: A survey of hysteresis, remanence and rock magnetic parameters, *J. Geophys. Res.* 102 (1997) 17659–17677.
- [2] R. Day, M. Fuller, V.A. Schmidt, Hysteresis properties of titanomagnetites: grain-size and compositional dependence, *Phys. Earth Planet. Inter.* 13 (1977) 260–267.
- [3] T. v. Dobeneck, A systematic analysis of natural magnetic mineral assemblages based on modelling hysteresis loops with coercivity-related hyperbolic basis functions, *Geophys. J. Int.* 124 (1996) 675–694.
- [4] E. Wohlfarth, Relations between different modes of acquisition of the remanent magnetization of ferromagnetic particles, *J. Appl. Phys.* 35 (1958) 595–596.
- [5] D. Dunlop, Theory and application of the Day plot ( $M_{rs}/M_s$  versus  $H_{cr}/H_c$ ) 1. theoretical curves and tests using titanomagnetite data, *J. Geophys. Res.* 107 (2002) 10.1029/2001JB000486.
- [6] D. Dunlop, Theory and application of the Day plot ( $M_{rs}/M_s$  versus  $H_{cr}/H_c$ ) 2. application to data for rocks, sediments, and soils, *J. Geophys. Res.* 107 (2002) 10.1029/2001JB000487.
- [7] M.J. Jackson, H.-U. Worm, S.K. Banerjee, Fourier analysis of digital hysteresis data: rock magnetic applications, *Phys. Earth Planet. Inter.* 65 (1990) 78–87.
- [8] A.P. Roberts, C.R. Pike, K.L. Verosub, First-order reversal curve diagrams: A new tool for characterizing the magnetic properties of natural samples, *J. Geophys. Res.* 105(B12) (2000) 28461–28475.
- [9] C.R. Pike, A.P. Roberts, M.J. Dekkers, K.L. Verosub, An investigation of multi-domain hysteresis mechanisms using FORC diagrams, *Phys. Earth Planet. Inter.* 126 (2001) 11–25.
- [10] T. von Dobeneck, *Neue Ansätze zur Messung und Interpretation der magnetischen Hysterese von Tiefseesedimenten*, Verlag Marie L. Leidorf, Buch am Erlbach, 1993.
- [11] P. Vlag, P. Rochette, M.J. Dekkers, Some additional hysteresis parameters for a natural (titano)magnetite with known grain size, *Geophys. Res. Lett.* 23 (1996) 2803–2806.
- [12] H.-U. Worm, Time dependent IRM: A new technique for magnetic granulometry, *Geophys. Res. Lett.* 26 (1999) 2557–2560.
- [13] D. Krása, R. Leonhardt, N. Petersen, Experimental procedure to detect multidomain remanence during Thellier-Thellier experiments, *Phys. Chem. Earth* (2003) in press.
- [14] A. Zitzelsberger, E. Schmidbauer, Magnetic properties of synthetic milled and annealed titanomagnetite ( $\text{Fe}_{2.3}\text{Ti}_{0.7}\text{O}_4$ ) particles 1–125  $\mu\text{m}$  in diameter and analysis of their microcrystalline structure, *Geophys. Res. Lett.* 23 (1996) 2855–2858.
- [15] L. Tauxe, T.A.T. Mullender, T. Pick, Potbellies, wasp-waists, and superparamagnetism in magnetic hysteresis, *J. Geophys. Res.* 101 (1996) 571–583.
- [16] A. Roberts, C. Yulong, K. Verosub, Wasp-waisted hyste-



- resis loops: minerals magnetic characteristics and discrimination of components in mixed magnetic systems, *J. Geophys. Res.* 100(B9) (1995) 17, 909–17, 924.
- [17] G. Muttoni, ‘Wasp-waisted’ hysteresis loops from a pyrrhotite and magnetite-bearing remagnetized Triassic limestone, *Geophys. Res. Lett.* 22 (1995) 3167–3170.
- [18] L. Xu, R. VanderVoo, D.R. Peacor, R.T. Beaubouef, Alteration and dissolution of fine grained magnetite and its effects on magnetization of the ocean floor, *Earth Planet. Sci. Lett.* 151 (2002) 279–288.
- [19] J. Gee, D.V. Kent, Calibration of magnetic granulometric trends in oceanic basalts, *Earth Planet. Sci. Lett.* 170 (1999) 377–390.
- [20] L. Néel, Théorie du traînage magnétique des ferromagnétiques en grains fins avec applications aux terres cuites, *Ann. Geophys.* 5 (1949) 99–136.
- [21] D. Dunlop, Viscous magnetization of 0.04–100  $\mu\text{m}$  magnetites, *J. Geophys.* 74 (1983) 667–687.